HF RFID Spiral Inductor Synthesis and Optimization

Nikola Gvozdenovic[1], Ralph Prestros[2], Christoph F. Mecklenbräuker[1]
[1] Christian Doppler Lab for Sustanable Mobility
Institute of Telecommunications, Vienna University of Technology, Austria
[2]NXP Semiconductors Austria GmbH, Austria
Email: nikola.gvozdenovic@tuwien.ac.at

***Abstract*—In this contribution, we discuss a planar spiral inductor synthesis method which generates physical dimensions of a HF RFID inductor according to the specified equivalent circuit parameters. A numerical model for spiral coil based on the partial element equivalent circuit (PEEC) method is combined with nonlinear optimization algorithm to optimize and synthesize coils. The main application is a HF RFID standard antenna for 13.56 MHz. The paper is intended as a manual for designing a HF RFID tag and includes procedure for measuring impedance of coils and chip, and simple fitted formulas for quick calculation of coil parameters in order to achieve required resonance frequency.**

***Index Terms*—PEEC, HF RFID, spiral coil**

I. Introduction

Contact-less chip cards, defined in [1] are used in a variety of applications. Notable implementation of these cards is in electronic ticketing systems, biometric passports, for identification as HF RFID (high-frequency radio frequency identification), in smart phones as NFC (near-field communication), etc.

Frequency of operation is 13.56 MHz and the information is transmitted through magnetic coupling. A card consists of an integrated circuit (IC) and an antenna. As antenna a planar spiral inductor (coil) is used. Additionally, a capacitor can be used for tuning. For designing a card, a good model of both the coil and the chip is essential.

In comparison to resistors and capacitors, inductors are the least ideal element and hardest to model accurately. Simple empirical formulas give values for the inductance that are of the same order of magnitude of the real inductance. Grover[2] gives working formulas and tables for inductance calculation of various inductors. In [3], formulas for various shapes of planar spiral coils of integrated inductors are presented, as well as in [4]. In this contribution we propose a simple method for finding coefficients for Wheeler and monomial formula of coil inductance.

For enhanced accuracy it is necessary to model the coil electromagnetically. Thin wires are best modeled by the partial element equivalent circuit (PEEC) method, cf. [5]. Antenna design of the rectangular spiral coils used in HF RFID is analyzed in depth in [6], using PEEC EM model.

For the circular spiral coils in [7] the N-turn spiral is approximated by N coaxial loops. Artillan et al.[8] implemented a PEEC model for circular spiral coils. In our recent paper [9] we analyze and measure circular spiral coils. Concerning coil synthesis, in [10] a method for coil synthesis combined with PEEC simulator is presented.

In contrast to the existing literature, we focus on the HF RFID antenna model for frequencies ranging from DC up to 500 MHz and compare the PEEC-based numerical model with the results obtained from an HFSS simulation, and with impedance measurements of manufactured coils.

Impedance of UHF RFID (ultra high frequency RFID) chips is measured and analyzed by Nikitin et al. in [11], and in [12]. Chip measurement and analysis of HF RFID chips, on the other hand, is presented in [13]. In both contributions chip impedance is found from S_{11} measurement using the reflection method.

Our approach is to use series method. The chip's impedance is extracted from an S_{21} measurement. Additionally, we also measure signals that are generated by the chip at harmonic frequencies.

This paper is organized as follows: in Sec. II we explain elements of HF RFID tag. In Sec. III we document our implementation of the PEEC model for circular coils where from the coil geometry we obtain circuit parameters(equivalent R and L). In Sec. IV we discuss how to synthesis coil, i.e. finding geometry of a coil for a target value of the coil inductance. Measurement of coil inductance and non-linear behavior of a chip are given in Sec. V, and VI respectively. Before we conclude, we discuss how to design a HF RFID tag in Sec. VII.

II. HF RFID tag analysis

An equivalent circuit model commonly used for HF RFID tags [14][15] is shown in Fig. 1. Elements of this model are:

- equivalent model of a coil consisting of serial inductance L_s, resistance R_s and parallel capacitance C_p
- input capacitor C_{In} for tuning the coil,
- full-wave rectifier (consisting of diodes like in Fig. 1 or of transistors),
- shunt voltage regulator for stabilizing the internal DC voltage,
- capacitor C_{TP} for storing the DC charge, and
- resistor R_L as the load of the digital circuitry.

We use this model for checking our measurement results. From our measurements and simulations we concluded that this is appropriate model of a tag.

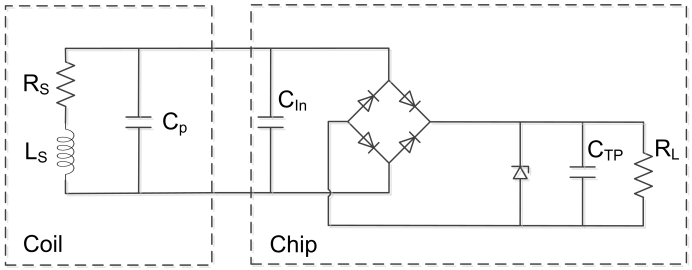

Fig. 1: Non-linear integrated circuit model [14].

III. EM MODEL OF SPIRAL COILS

The main idea of the PEEC method is to divide a conductor's volume and surface into mutually interconnected cells. Volume cells are called filaments and surface cells are called panels. We used the same approach as in [6] with unequal size of filaments to better model skin and proximity effects. The dimension of the smallest filament (at the edge of conductor) is chosen to be in the order of the magnitude of the skin depth. Since the skin depth on 13.56 MHz is 17 μm and conductor is usually thin (typically made of wire with 80 μm diameter) it is not required to have large number of filaments.

The size of HF RFID coil is specified in the standard [1]. As shown in Fig. 2 two commonly used geometries of coils are rectangular and circular, produced from wire(rectangular cross-section) or on PCB (rectangular cross-section).

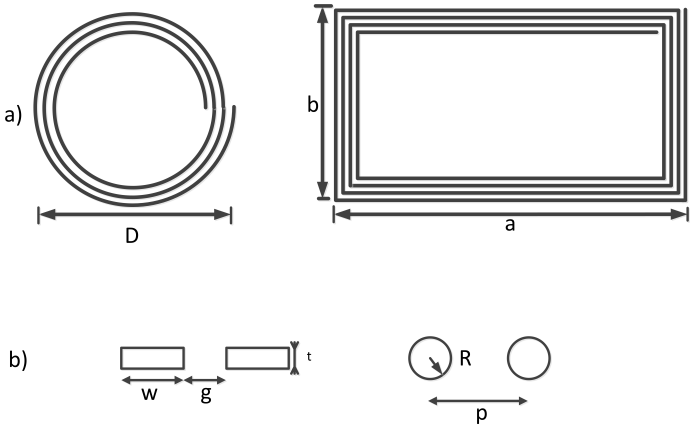

Fig. 2: Four types of coils. Two types of geometry (circular or rectangular) and two types of cross-section (circular or rectangular).

For the circular spirals, as in [8] we approximate N-turn spiral with N coaxial loops. Each loop is then divided in circular filaments(one or more). The parameters of the i-th filament of the circular spiral coil are:
r_i, $r_{i\text{int}}$, $r_{i\text{ext}}$ - median, inner an outer radius;
w_i,t_i - width and thickness, and z_i - position in the z direction.
Then, resistances of the filaments are calculated by:

$$R_i = \frac{2\pi}{\sigma t_i \ln(\frac{r_{i\text{ext}}}{r_{i\text{int}}})} \tag{1}$$

Self-inductance of each filament is calculated according to Grover's formula for a single loop with rectangular cross-section:

$$L_i = 4\pi 10^{-7} r_i \big(\frac{1}{2}(1+\frac{1}{6}c_a^2)\ln\frac{8}{c_a^2} - 0.84834 + 0.2041c_a^2\big) \tag{2}$$

$$c_a = \frac{w_i}{2r_i} \tag{3}$$

Mutual inductance between i-th and j-th filament is calculated according to the approximative Neumann's formula [16]:

$$M_{ij} = 4\pi 10^{-7}\big(-1.5589 - 1.3765\ln\log k\big)\sqrt{\frac{r_i r_j}{8}} \tag{4}$$

$$k = \frac{r_i^2 + r_j^2 + h^2}{2r_i r_j}; h = |z_i - z_j| \tag{5}$$

Rectangular inductors, on the other hand, are first divided in segments (four in each turn) and then in filaments that have same length as segments. Consequently, resistance and inductance of filaments is calculated as following.

Resistance of a filament is calculated as:

$$R_i = \frac{l_i}{\sigma w_i t_i} \tag{6}$$

where l_i,w_i and t_i are length, width and thickness of a filament i.

Self inductance of a filament i is calculated according to:

$$L_i = \frac{\mu}{2\pi} l_i (\ln\frac{2\mathrm{l_i}}{\mathrm{t_i}+\mathrm{w_i}} + 0.50049 + \frac{\mathrm{t_i}+\mathrm{w_i}}{3\mathrm{l_i}}) \tag{7}$$

For the mutual inductance between i-th and j-th filament there is three different cases, depending on the mutual position of filaments and direction of the current flow. For parallel filaments mutual inductance is constructive if currents flow in the same direction and destructive if in opposite. For orthogonal filaments we assume that mutual inductance is negligible. Numerically this can be expressed as:

$$M_{i,j} = \begin{cases} |M_{i,j}| & \| \text{ filaments,constructive} \\ -|M_{i,j}| & \| \text{ filaments,destructive} \\ 0 & \perp \text{ filaments.} \end{cases} \tag{8}$$

where

$$|M_{i,j}| = \frac{\mu}{2\pi} l_i [\ln(\frac{l_i}{d_{ij}} + \sqrt{1+\frac{l_i^2}{d_{ij}^2}}) - \sqrt{1+\frac{d_{ij}^2}{l_i^2}} + \frac{d_{ij}}{l_i}] \tag{9}$$

At the moment capacitance is only modeled with the simple analytical formulas as in [4]:

$$C = \frac{\pi\varepsilon_r\varepsilon_0}{\ln\frac{\mathrm{p-R}}{\mathrm{R}}} l_{coil} \tag{10}$$

for wire inductors and:

$$C = \frac{\varepsilon_r\varepsilon_0 w}{g\ln\frac{g+w}{g} + w\ln\frac{g+w}{w}} l_{coil} \tag{11}$$

for PCB inductors, where l_{coil} is total length of inductor (see appendix).

IV. Inductor synthesis and optimization

To design HF RFID tag it is also important to find out how to get from the electrical parameters of the coils to its geometrical parameters. To achieve this we used simple Wheeler formula for coil inductance:

$$L_{\mathrm{wh}} = K_1 \mu_0 \frac{N^2 d_{\mathrm{avg}}}{1 + K_2 \rho} \tag{12}$$

where values of coefficients K_1 and K_2 are obtained by curve fitting : K_1=1.9345 and K_2=4.0241 for circular geometry, and K_1=3.6773 K_2=9.86 for rectangular geometry.
For circular coils d_{avg} is average diameter but for rectangular $d_{\mathrm{avg}}^{(r)} = \sqrt{ab}$.
Filling factor ρ is ratio between wiring width and average radius.

Coefficients K_1 and K_2 where extracted by curve fitting to the large number of measurement by following method:

$$L = \begin{bmatrix} \mu_0 N^2 d_{\mathrm{avg}} & -L\rho \end{bmatrix} \times \begin{bmatrix} K_1 \\ K_2 \end{bmatrix} \tag{13}$$

Then

$$K = (A^T A)^{-1} A^T L \tag{14}$$

Alternatively monomial formula for calculating coil inductance can be used:

$$L_{\mathrm{mn}} = \beta a^{\alpha_1} b^{\alpha_2} w^{\alpha_3} g^{\alpha_4} N^{\alpha_5}. \tag{15}$$

Here we assume exponential dependence to each of coil's geometrical parameters. As an example, coefficients α for rectangular wire conductors are summarized in Tab. I.

TABLE I: Coefficient of monomial formula

β	α_1	α_2	α_3	α_4	α_5
0.393	-0.874	0.674	0.182	-0.171	1.83

Based on Wheeler formula and dimension constrains we implemented Monte Carlo simulation of coil inductance because ρ is not independent variable (depends on N and d_{avg}). In Fig. 3 we show inductance versus d_{avg}. From this graph user can select desired dimension of a coil and inductance required for the tag.

In Fig. 4 we show inductance versus N. This figure is more illustrative, and we can conclude that coils with 3 and 4 turns have inductance smaller than 3 μH. To achieve 5μH we need large coil with 5 turns or average sized with 6.

For the coil synthesis we minimize function:

$$f(N, d_{\mathrm{avg}}, \rho) = K_1 \mu_0 N^2 d_{\mathrm{avg}} - (1 + K_2 \rho) L_{\mathrm{tg}} \tag{16}$$

For each value of $N \in [N_{\mathrm{MIN}} N_{\mathrm{MAX}}]$ we find values of d_{avg} and ρ for which this function is minimal. From this set of coils we select one that satisfies most of the requirements (closest to target value of L, has smallest diameter, etc.) and then do the final simulation with our coil analysis script.

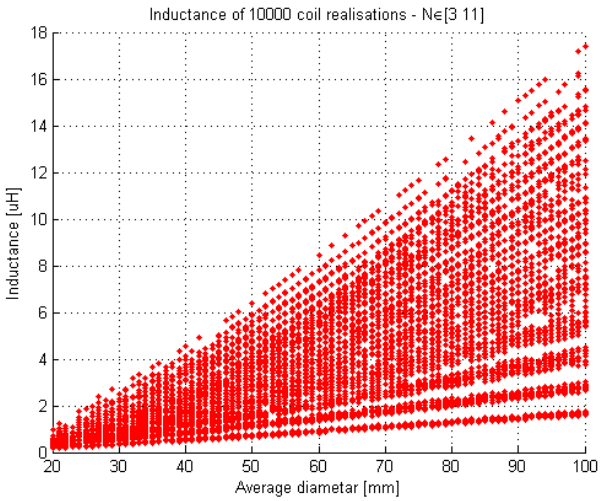

Fig. 3: Monte Carlo simulation of coil inductance versus average diameter d_{avg}.

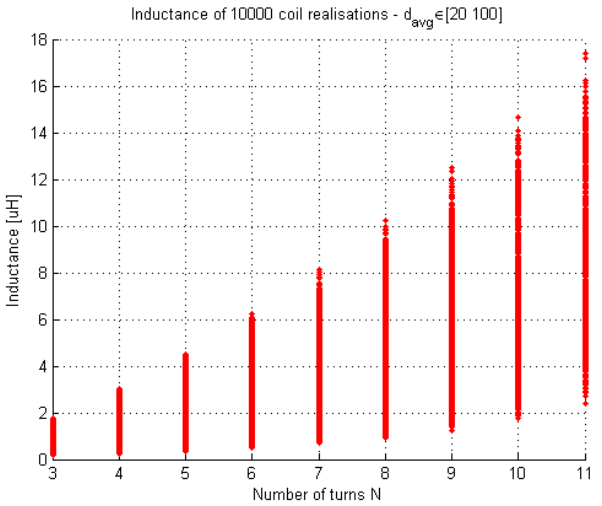

Fig. 4: Monte Carlo simulation of coil inductance L versus number of turns N.

V. Coil measurement and simulation

To investigate how different values of coil's geometrical parameters influence its electrical parameters, we made a set of 6 circular coils given in Tab. II. The coils are produced on RO4350 substrate, with a thickness of 0.51 mm. We did not use solder mask because it has some influence on wire capacitance between coil turns.

We measured with an Agilent 4395 A impedance analyzer with the RF impedance test adapter 43961A. A custom calibration kit was used to enable accurate fixture compensation. The measurement reference plane was shifted directly to the input of the coil antenna. A support made of dielectric material was used to hold the coil, so that the influence of the environment is minimal.

To check our simulator we modeled a spiral with $N = 4$ turns, $a = 10$ mm, $w = 0.5$ mm,and $g = 0.3$ mm. Metalization thickness is 35 μm. In Fig. 5 we show simulated impedance

of the coil vs. frequency. Fo the $RL||C$ equivalent circuit, final result for resistance and inductance of the first coil is $R_{eq} = 0.2759\,\Omega$ and $L_{eq} = 0.6416\,\mu$H, which is in a good agreement with the measurement results and HFSS simulation shown on the same figure. If we compare measured results with those obtained by PEEC and HFSS simulation, we observe that they are in a good agreement.

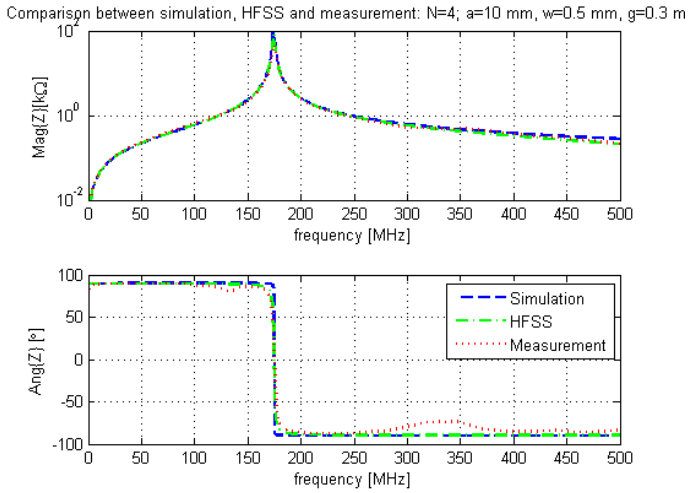

Fig. 5: Comparison between simulation, HFSS and measurement: N=4, a=10 mm, w=0.5 mm, g=0.3 mm, N=6.

The results acquired were used to extract a simple $RL||C$ equivalent circuit model. In Tab. II we summarize values of R, L and C of every coil measured. The simple equivalent circuit models the fundamental resonance with high accuracy. However, further resonances at frequencies above 200 MHz are not modeled. Some inaccuracies in the R, L and C values might also result from these higher resonances. In future work more detailed equivalent circuits will be used to better model higher resonances.

TABLE II: Parameters of circular coils produced on PCB

Coil No	a [mm]	w [mm]	g [mm]	N	C [pF]	R [Ω]	L [μH]
1	10	0.5	0.3	4	1.32	0.4	0.62
2	10	0.5	0.3	8	1.89	1.48	2.07
3	13	0.5	0.3	6	2.19	0.92	1.64
4	17	0.5	0.3	6	2.32	1.17	2.29
5	13	0.5	0.5	6	1.97	0.87	1.71
6	13	0.5	0.7	6	2.21	0.99	1.55

To evaluate how production influences the measured coil impedance, these coils are made twice. We observed that the variance of R, L and C between two sets are quit small and within the accuracy of the measurement device.

For the simulator verification of rectangular coil, on the same way a set of rectangular coils is produced. These coils are made of thin wire and also have different geometrical parameters: dimensions, wire pitch and number of turns, as shown in Tab. III.

In Tab. IV we compare measurement results with our EM simulator and the results obtained by simple Wheeler and monomial formula. We can observe that these results are in good agreement. Simple formulas would be used for quick calculation of coil inductance, but for the final verification our simulator would be used.

TABLE III: Parameters of rectangular coils made of wire

Coil No	a [mm]	b [mm]	d [μm]	p [mm]	N	C [pF]	R [Ω]	L [μH]
7	80.5	48.5	80	0.4	3	4.5	3.7	1.9
8	80.5	48.5	80	1	3	3.4	6.6	1.6
9	80.5	48.5	80	1.4	3	5.4	5.2	1.4
10	78.6	23	80	0.6	4	3.6	4.7	1.9
11	80.5	48.5	80	0.5	5	3.8	6.1	4.8
12	80.5	48.5	80	1	5	4.2	9.3	3.8

TABLE IV: Comparison between measurement, curve fitting and EM simulator

Coil No	L_{mes} [μH]	L_{sim} [μH]	L_{wh} [μH]	L_{mn} [μH]
1	0.62	0.7	0.59	0.62
2	2.07	2.5	2.09	2.1
3	1.64	1.9	1.67	1.69
4	2.29	2.6	2.29	2.26
5	1.71	1.9	1.62	1.62
6	1.55	1.8	1.58	1.58
7	1.9	2.2	2.27	2.25
8	1.6	1.8	2	1.8
9	1.4	1.7	1.64	1.64
10	1.9	2.6	2.24	2.2
11	4.8	6.3	5.4	5.5
12	3.8	6	4.7	4.9

VI. Chip non-linearity measurement

In this section we discuss measurement and modeling of non-linearity of HF RFID chips. We present only parts of the procedure which are important for the tag design. More details on the measurement are given in [17].

Since it is expected that chip has high input impedance reflection method is prone to error. Consequently we used series measurement setup proposed in [18] to measure chip's impedance as well as amplitude of harmonics produced by the chip.

The circuit of this measurement setup is shown in Fig. 6a. The advantage of this approach is that the load situation is defined at all frequencies. At the fundamental frequency the chip is powered by a source with an equivalent source impedance of $100\,\Omega$, and at all harmonic frequencies the chip is terminated with a load of $100\,\Omega$.

The current and voltage are obtained by solving the measurement circuit shown in Fig. 6a according to the following expressions:

$$\underline{U} = \underline{U}_s - 2\underline{U}_2 \tag{17}$$

$$\underline{I} = \frac{\underline{U}_2}{Z_0}. \tag{18}$$

Commonly used harmonic model for full wave rectifier circuit is shown in Fig. 6b. Due to rectification chip behaves as current controlled current source. It produces harmonic currents on the AC sides which are controlled by DC current inside the chip.

$$i_s(t) = \sum_{n=1,3,5,\ldots}^{\infty} \frac{4}{n\pi} I_d \sin(n2\pi f_0 t) = i_{sf}(t) + i_{sh}(t) \quad (19)$$

We analyze the chip's response at the fundamental and odd numbered harmonic frequencies ($3f_0, 5f_0$ etc.) as a function of the available power at the fundamental frequency of $f_0 = 13.56$ MHz. Impedance is calculated from the S_{21} measurement at the fundamental. The generated harmonics are related to the incoming wave at port 2 of the VNA (b_2).

For the measurements we use a ZVA8 VNA by Rohde&Schwarz which is controlled by Matlab through VISA interface. VNA generates signal at the port 1 on the fundamental frequency on the specific power level. This signal is amplified to increase the range of the signal. Since the amplifier and VNA itself induce harmonics, a custom designed low-pass filter (LPF) is used that also provides an impedance of 50 Ω for all harmonics produced by DUT. For accurate calibration of this measurement a custom test fixture and calibration kit were designed.

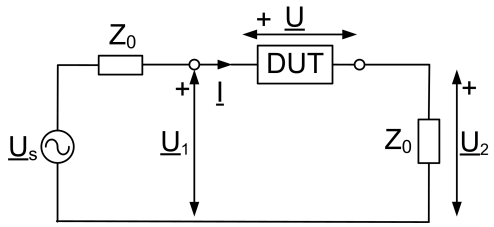

(a) Proposed measurement approach.

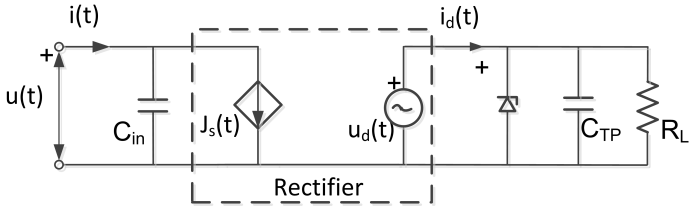

(b) Simplified harmonic model of a chip.

Fig. 6: Proposed measurement setup and simplified harmonic model of a chip.

To find the chip impedance, first we measure the S_{21}-parameter at the fundamental frequency versus power. We calculate the chip's fundamental impedance according to:

$$Z_{\text{chip}} = \frac{2Z_0(1 - S_{21})}{S_{21}}. \quad (20)$$

In Fig. 7 we show the equivalent parallel conductance and capacitance vs source power in a range from 0 to 5 V for four different chips. G_p and C_p are calculated from:

$$G_p = \text{Re}\{1/\text{Z}_{\text{chip}}\} \quad (21)$$
$$C_p = \text{Im}\{1/\text{Z}_{\text{chip}}\}/\omega_0. \quad (22)$$

From the figure we can see that there is small variation in the behavior of the 4 chips. We also observe different regions of the operation of the chip depending on the available power:

- available power below 1.5 V - rectifier is not conducting - G_p and C_p constant (small conductivity, C_p around 15 pF)
- available power in the range above 1.5 V - rectifier is operating.

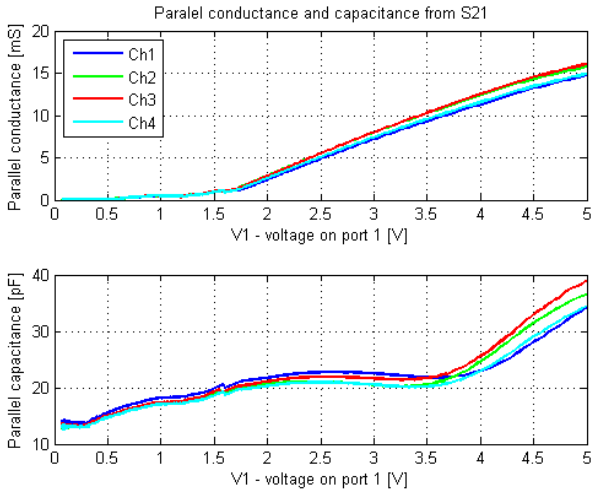

Fig. 7: Conductance and capacitance of the equivalent G_p and C_p calculated from S_{21}.

Now we investigate the harmonic signals generated by the chip as a function of available input power. We calculate currents produced by the chip from the S21 on the fundamental frequency and from the ratio of b_2 and a_1 on the harmonics as described before.

In Fig. 8 we show currents produced by a chip on the fundamental frequency and on the first 7 odd numbered harmonics. We can observe quick increase of current on f_0 starting from 1.5 V, due to typical behavior of the rectifier.

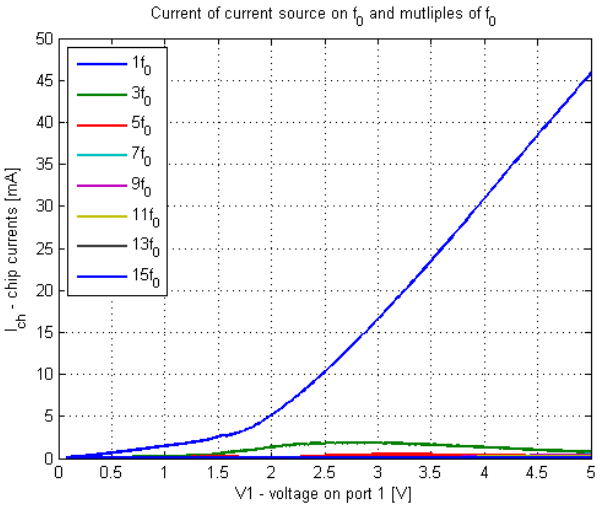

Fig. 8: First seven odd harmonics produced by a chip.

Fig. 9 is more illustrative for harmonics frequencies. We can see that this currents are quite strong. The strongest third harmonics reaches 1.8 mA when available power is 3 V.

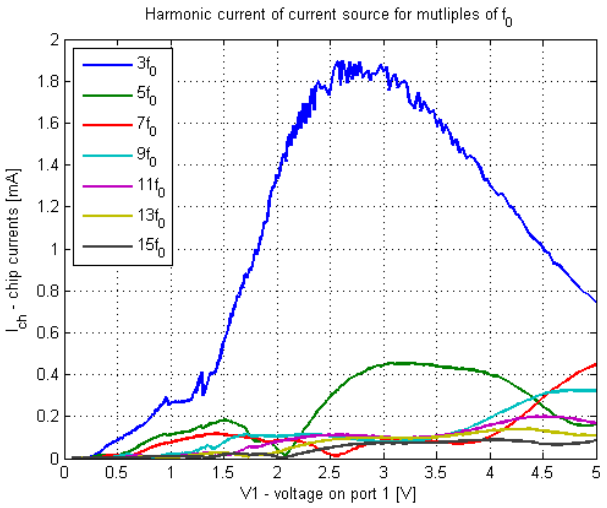

Fig. 9: First seven odd harmonics produced by a chip.

VII. HF RFID TAG DESIGN

After detail analysis of HF RFID coil and chip in this section we discuss how to design HF RFID tag to fulfill the requirements. Most important parameter of a HF RFID tag is resonance frequency that can be found from:

$$\omega_{\text{res}} \approx \frac{1}{\sqrt{L_s C_{tot}}} \tag{23}$$

where $C_{tot} = C_p + C_{ch}$. We can see that three parameters that influence resonant frequency of a tag are inductance and parasitic capacitance of a coil, and capacitance of a chip. In Fig. 10 we show target value of inductance versus chip impedance in order to achieve target value of resonance frequency. From the previous section we observe that our chip has 17 pF capacitance. Most of the practically used coils have capacitance around 4 pF. From Fig. 10 we see that our target inductance value should be $5\mu H$.

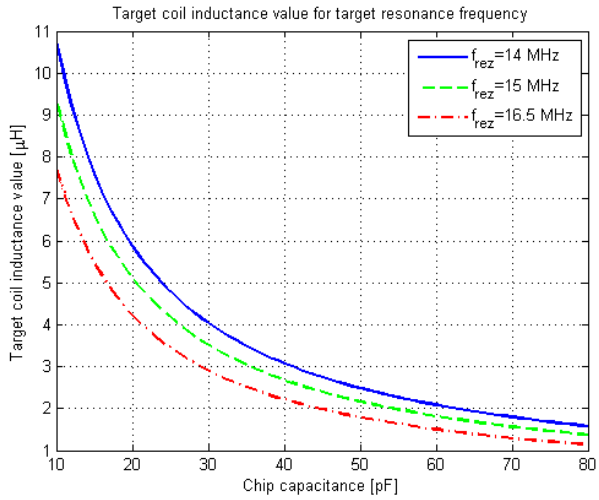

Fig. 10: Target inductance for the target resonance frequency depending of the chip's impedance.

Then we implement algorithm from Sec. IV by minimizing function in Eq. 16 to find most suitable coil. From more solution offered we pick one with 5 turns and geometrical mean dimension of 60 mm. This criteria is fulfilled by class 1 coils. Example is a coil with dimensions 80.5 x 48.5 mm.

VIII. CONCLUSIONS AND FUTURE WORK

In this contribution, we discuss a planar spiral inductor synthesis method which generates physical dimensions of the HF RFID inductor according to the specified equivalent circuit parameters. A numerical model for spiral coil based on the partial element equivalent circuit (PEEC) method is combined with nonlinear optimization algorithm to optimize and synthesize coils. Both HF RFID coil and chip are evaluated by measurements, and optimization simulator is used for the design of HF RFID tag.

For the future work we will verify our approaches on the large number of coil simulated in commercially available EM simulators. Furthermore we will include load modulation in our consideration.

APPENDIX A
MATHEMATICAL REPRESENTATION OF SPIRAL COILS' GEOMETRIES

Here we mathematically describe geometry of circular and rectangular spiral coils with rectangular cross-section. For coils made of wire (circular cross-section) in the formulas below only change is instead of $g + w$ it should be written wire pitch p.

Circular spiral coil can be mathematically described by:

$$r = a + (g + w) \cdot \frac{\theta}{2\pi} \tag{24}$$

$$x = (a + (g + w) \cdot \frac{\theta}{2\pi}) cos\theta \tag{25}$$

$$y = (a + (g + w) \cdot \frac{\theta}{2\pi}) sin\theta \tag{26}$$

where a is the starting radius of the spiral, w the wire conductor width, g the gap between turns and $\theta \in [0, 2N\pi)$. Consequently coil length and outer diameter are calculated as:

$$l_{coil} = 2Na\pi + N^2\pi(g + w) \tag{27}$$

$$D_{out} = 2[a + (N + 1/4)(g + w)] \tag{28}$$

Corners of rectangular spiral lie on an elliptic spiral. The position of this corners can be mathematically described as:

$$x_{cr} = (a_{el} + (g + w) \cdot \frac{\theta}{2\pi}) \cos\theta \tag{29}$$

$$y_{cr} = (b_{el} + (g + w) \cdot \frac{\theta}{2\pi}) \sin\theta \tag{30}$$

where angle θ is defined as

$$\theta \in [\frac{\pi}{4} : \frac{\pi}{2} : 2N\pi + \frac{\pi}{4}) \tag{31}$$

and $a_{el} = a_{in} \cdot \sqrt{2}$, and $b_{el} = b_{in} \cdot \sqrt{2}$ (a_{in} and b_{in} inner dimension of a rectangular coil). Length of segment is then calculated as Euclidean distance of two consecutive corners, and length of coil l_{coil} is then sum of all segment lengths.

Then position of segments is defined as a central point of a segment:

$$p_{\mathrm{sg_i}} = \left[\frac{x_{\mathrm{cr_i}}+x_{\mathrm{cr_{i+1}}}}{2}\,\frac{y_{\mathrm{cr_i}}+y_{\mathrm{cr_{i+1}}}}{2}\right] \tag{32}$$

Distance between segments is then defined as Euclidean distance between two corresponding segment positions.

APPENDIX B
FITTING METHOD FOR MONOMIAL COEFFICIENT EXTRACTION

Monomial expression of coil inductance is:

$$L_{\mathrm{mn}} = \beta a^{\alpha_1} b^{\alpha_2} w^{\alpha_3} g^{\alpha_4} N^{\alpha_5} \tag{33}$$

For better fitting we do a $\log$ of this equation:

$$\begin{aligned} y = \log L_{\mathrm{mn}} &= \log\beta + \alpha_1 \log a + \alpha_2 \log b \\ &+ \alpha_3 \log w + \alpha_4 \log g + \alpha_5 \log N \end{aligned} \tag{34}$$

$$y = \alpha_0 + \alpha_1 x_1 + \alpha_2 x_2 + \alpha_3 x_3 + \alpha_4 x_4 + \alpha_5 x_5 \tag{35}$$

Now if we have a set of measured values of L of a coils with known geometry we can write previous equation in matrix form:

$$\mathbf{y} = \alpha \mathbf{x} \tag{36}$$

Vector α we find by solving previous matrix equation:

$$\alpha = \mathbf{y}\mathbf{x}^T(\mathbf{x}\mathbf{x}^T)^{-1} \tag{37}$$

The same approach we used for both coil geometries and also for R and C and we found good agreement between analytical and measured values. Values of monomial coefficients for different quantities of circular and rectangular coils from Sec. V are summarized in Tab. V and Tab. VI respectively.

$$K_{\mathrm{mn}} = \beta a^{\alpha_1} w^{\alpha_2} g^{\alpha_3} N^{\alpha_4}. \tag{38}$$

TABLE V: Monomial coefficients for circular coils

Quantity K	β_l	α_{l1}	α_{l2}	α_{l3}	α_{l4}
L[μH]	0.003	1.1	-0.39	-0.08	1.76
R[Ω]	0.0043	0.59	-0.85	-0.013	1.95
C[pF]	0.18	0.81	0.55	0.12	0.46

$$K_{\mathrm{mn}} = \beta a^{\alpha_1} b^{\alpha_2} w^{\alpha_3} g^{\alpha_4} N^{\alpha_5}. \tag{39}$$

TABLE VI: Monomial coefficients for rectangular coils

Quantity K	β	α_1	α_2	α_3	α_4	α_5
L[μH]	0.393	-0.874	0.674	0.182	-0.171	1.83
R[Ω]	0.4815	-0.13	0.33	0.04	0.005	0.89
C[pF]	0.69	0.66	0.29	-0.69	-0.28	0.3

ACKNOWLEDGMENT

This work has been funded by the Christian Doppler Laboratory for Wireless Technologies for Sustainable Mobility, the Federal Ministry of Economy, Family and Youth and the National Foundation for Research, Technology and Development of Austria and by our industrial partner NXP Semiconductors Austria GmbH. We thank dr Lukas W. Mayer for his help with the measurements and prof. dr Markus Rupp for discussions and ideas.

REFERENCES

[1] *Identification cards- Contactless integrated circuit cards - Proximity cards*, ISO/IEC Std. 14 443-1, 2008.
[2] F. Grover, *Inductance calculations*. Dover publications, 2004.
[3] S. S. Mohan, "The design, modeling and optimization of on-chip inductor and transformer circuits," Ph.D. dissertation, Department of Electrical Engineering, Stanford University, 1999.
[4] W. Lin, "Modellierung, Optimierung und Vermessen von HF-RFID-Transpondern unter bercksichtigung nichtlinearer Effekte," Ph.D. dissertation, Faculty of Electrical Engineering and Computer Science, Leibniy Universitt Hannover, 2012.
[5] M. Kamon, N. Marques, L. Silveira, and J. White, "Automatic generation of accurate circuit models of 3-D interconnect," *Components, Packaging, and Manufacturing Technology, Part B: Advanced Packaging, IEEE Transactions on*, vol. 21, no. 3, pp. 225 –240, aug 1998.
[6] P. Scholz, "Analysis and numerical modeling of inductively coupled antenna systems," Ph.D. dissertation, Theorie Elektromagnetischer Felder (TEMF), 2010.
[7] B. Rejaei, "Mixed-potential volume integral-equation approach for circular spiral inductors," *Microwave Theory and Techniques, IEEE Transactions on*, vol. 52, no. 8, pp. 1820 – 1829, aug. 2004.
[8] P. Artillan, B. Estibals, and C. Alonso, "A new modeling approach for circular spiral inductors," in *Power Electronics and Applications, 2007 European Conference on*, sept. 2007, pp. 1 –8.
[9] N. Gvozdenovic, L. Mayer, R. Prestros, C. Mecklenbruker, and A. Scholtz, "PEEC modeling of circular spiral coils," in *European Microwave Conference*, 2013.
[10] H.-C. Lu, T. Chan, C. Chen, C.-M. Liu, H.-J. Hsing, and P.-S. Huang, "Ltcc spiral inductor synthesis and optimization with measurement verification," *Advanced Packaging, IEEE Transactions on*, vol. 33, no. 1, pp. 160–168, Feb 2010.
[11] P. Nikitin, K. V. S. Rao, R. Martinez, and S. Lam, "Sensitivity and impedance measurements of UHF RFID chips," *Microwave Theory and Techniques, IEEE Transactions on*, vol. 57, no. 5, pp. 1297–1302, 2009.
[12] W. L. Mayer, "Antenna design for future multi-standard and multi-frequency RFID systems," Ph.D. dissertation, Faculty of Electrical Engineering and Information Technology, VIenna University of Technology, 2009.
[13] M. Gebhart, J. Bruckbauer, and M. Gossar, "Chip impedance characterization for contactless proximity personal cards," in *Communication Systems Networks and Digital Signal Processing (CSNDSP), 2010 7th International Symposium on*, 2010, pp. 826–830.
[14] W. Lin, B. Geck, and H. Eul, "Optimization of NFC compatible transponder with respect to the nonlinear IC impedance," in *Wireless Sensing, Local Positioning, and RFID, 2009. IMWS 2009. IEEE MTT-S International Microwave Workshop on*, 2009, pp. 1–4.
[15] K. Finkenzeller, *RFID-Handbuch: Grundlagen und praktische Anwendungen von Transpondern, kontaktlosen Chipkarten und NFC*. Hanser, 2008. [Online]. Available: http://books.google.at/books?id=49HTBDrfqFUC
[16] H. Chan, K. Cheng, and D. Sutanto, "A simplified neumann's formula for calculation of inductance of spiral coil," in *Power Electronics and Variable Speed Drives, 2000. Eighth International Conference on (IEE Conf. Publ. No. 475)*, 2000, pp. 69 –73.
[17] N. Gvozdenovic, L. W. Mayer, and C. F. Mecklenbrauker, "Measurement of harmonic distortions and impedance of HF RFID chips," in *8th European Conference on Antennas and Propagation, euCap 2014*, 2014.
[18] *Impedance Measurements - Evaluating EMC Components with DC Bias Superimposed*, Agillent Technologies.